International Research Journal of Engineering and Technology (IRJET) e-ISSN: 2395-0056
Volume: 08 Issue: 04 | Apr 2021 www.irjet.net p-ISSN: 2395-0072

Solar powered hand held ULV sprayer

El-Bialee, N.M.

Senior Researcher of Agric. Bio. Eng. Sys. Res. Department. Agric. Engineering Res., Inst. (AEnRI)., Agric. Res. Center (ARC)., Giza. Egypt.

Abstract: *This paper mainly focuses on the concept known as Solar Power Sprayer. The regular hand held ULV spinning cone sprayer, Ulva+ brand, which used to apply the agrochemicals liquids, is converting to a solar powered sprayer system "SSS". To process its shortcomings, i.e., irregular deposition intensity, high running cost, power limited, and a great pollution due to disposal the batteries. The concoction is accomplished by the use of; two modules of the solar photovoltaic panels "SPV" (2175 and 3600cm^2), and the control unit. The SSS operates in three modes; solar radiation, rechargeable battery, and hyper. The climatic season 2018-2019 data, were analyzing, to predict the theoretical performance of the SSS. Therefore, it tested and evaluated technically, also economically. Based on experiments, it is found that, the RB full charge time has a direct relation with the operating power "O_P" and opposite relations with both of the SPV area and the solar operating time. In contrast, of the total operating time "TOT". Without SPV, the sprauing process "SP" can be done with a constant O_P of 12, 18 and 22W for a minimum period of 3.7, 2.47, and 2.02 h, respectively. Furthermore, results show that, the O_P has a height significant effect ($P \leq 1\%$) on the droplet deposition intensity, while, the operating mode was insignificant. The SSS power cost was more economical, with regularity distribution, and had long TOT.*

Keywords: ULV hand held sprayer, Solar energy, Panel.

I. Introduction

In the last decade, the Egyptian farmer faces many obstacles, that threaten his continuation in agricultural activity, i.e., increasing the costs of agricultural inputs (seeds, fertilizers, and….etc..), as a direct result of the Egyptian currency floatation, and lifting subsidies on petroleum products (fuel), in addition to other problems.
While, achieving profitability, with self-sufficiency in food, are the most important goals of agriculture profession. In addition, profitability can be achieved through increasing productivity and reducing production costs. Increasing productivity is achieved through many tasks, including a spraying process "SP" to disease and weed control, fertilization,...etc. Whereas, converting the power source to solar energy in some agricultural production process, leads to significantly reduce both of the cost and pollution.
A sprayer is an equipment used to spray the agrochemical liquids (fertilizers, insecticides, pesticides,...etc.) easily and quickly to the crops, in order to supply the plant with nutrients, avoid any pest, and control the weeds, as a means of crop quality control [1].

Agrochemical liquids, e.g., pesticide dose, must be applied with care. Where, about 50-80% of applied pesticide is wasted due to poor spray machinery and inappropriate application methods [2]. So, the right dose prevents yield losses up to 45% [3]. Since under dose may not give the desired coverage and resistance of pests. Whereas, overdose is increasing on farm production expenses, environmental contamination and phyto- toxicity (may contaminate the edible parts through residues) to humans and other species [4].

Improving liquid application quality and efficiency, i.e., the droplet sizes spectrum, the liquid distribution uniformity throughout the crop field, the host plant coverage, and control the chemical distribution on the plant surface, are an important topic of SP [5,6,7]. Where, the sprayer, which gives a high number of droplets cm^{-2}., of the host plant, will be better comparing the others [8]. Considering the above requirements, many researchers have developed different types of sprayer [9,10,11,12].

Two main types of sprayer were used in spraying task; A) hand-operated spray pump, B) motorized sprayer pump. The main impediment of the first type gives a discharge (0.8-1.5Lmin^{-1}). Where, the labor operates the sprayer, till the pesticides are deposited by a sufficient amount. Another, obstacle is resulting in harmful effects on the laborer, Where, the laborer gets tired after 5-6h of continuous work [13,14]. While, the other type gives a discharge (6 - 8Lmin^{-1}) which leads to wastage of chemical liquid, and requires more fuel which is expensive. Therefore, increases the running cost of the SP. Also, it exhausts CO_2 as a pollutant that is, which has a harmful to the environment (greenhouse effect), and human health [15].

In this context, some predictions indicate that reserves of oil, coal and natural gas were deplete within 34–40, 106–200, and 36–70 years, respectively [16]. These predictions have encouraged a renewable energy as a power source in state of conventional fuel, especially at agriculture profession.

Renewable energy is an energy which comes from natural resources, i,e., sun, wind, hydro, tides (offshore wind - wave- marine current - ocean thermal energy conversion- tidal power- osmotic power), and geothermal heat. In addition, biomass (oil from plants, wood from sustainable sources, and biogas from fermentation of manure and crop residues). In this context, these energies are clean, risk-

free and constitute no harm to man and the environment [17,18].

The sun is the main source of all energy on the earth, where, they draw their strength from it. It is most abundant, inexhaustible and universal source of energy, [19]. In addition, the solar energy level is in line with air , it is free, unlimited, free from pollution, does not create greenhouse gases, nor does it create waste that must be stored[20, 21]. On the surface of the solar photovoltaic panel "SPV", the solar radiation "RS" harvested and converting energy photon to electric energy. It consists of multi arrays of solar cells, crafted from silicon semiconductor. They connected together in series and parallel, to creating the appropriate voltage and current [22]. While, by capture heating systems techniques, it converted to heat [23,24].
Egypt belongs to the global Sunbelt [25]. Where, the sunshine duration extends to 2300-4000h $year^{-1}$ (9- 11h day^{-1} with approximately 325 days $year^{-1}$), with of 5 - 8 kWh m^{-2} day^{-1} [26]. Consequently, Egypt's economically viable solar potential in the range of 74 PWh$year^{-1}$ [27]. So, it can save money or even sold it as a cash crop, increasing self-reliance, reducing pollution. Also, it can be utilized in miscellaneous application at agriculture areas like, solar home, solar dryer for agricultural products (crop, grain, vegetable and fruit), drying poultry manure, human and animal feed solar cooker, water pumping, solar greenhouse, and solar photovoltaic operated equipment for plant-protection (Solar photovoltaic sprayer and duster), and other agriculture equipment, i.e., milling machine and disk mower, [28, 29, 30, 31, 32, 33]. Like most renewable energy sources, the solar energy also has some disadvantages, where, it is an intermittent energy source and has time limitations. Over and above, solar power generation varies, by season, location, daytime, solar radiation, temperature and variation in weather, [34]. So, solar energy storage is an important issue, to keep continuous availability by providing storage energy during these low production or high demand times, and also limit the wasted solar energy [19].

Whatever, solar energy is stored in different forms, i,e., heat, electrical, chemical and mechanical [35]. Energy storage devices can be categorized as mechanical (Pumped hydro, compressed air and flywheels), chemical (Batteries of conventional, liquid Metal & Molten salt, metal air, flow and, fuel cells), electromagnetic (Superconductor magnetic, super-capacitor and capacitor /inductor), and thermal (Sensible, latent, and reversible chemical reaction) as mentioned by [36].

The Baghdad battery (248 BC–226 AD) may be the first attempt by a human to store energy in the chemicals form [37]. Then, followed by long time in the modern era, the innovation of the battery in its first images by Luigi Galvani (1737-1798) and Alessandro Volta (1745-1827).
A battery is a manner of storing energy in a chemical form, thereafter converting it to electrical energy again. It is an electrochemical device, with an anode, a cathode, an electrolyte and the external case. Where, the main difference between them is the materials used as electrodes and electrolyte. Typically, these batteries come in sizes AAA, AA, C, D and 9V [38]. Therefore, it can be classified depending on their utility to; primary or single use (cannot be recharged), e.g., Zinc carbon (ZnC- Alkaline batteries), Alkaline Manganese (AlMn), Zinc Air (ZnAir), Silver Oxide (AgO) and Lithium Manganese Dioxide ($LiMnO_2$), and secondary, or multiple use (rechargeable), e.g., Nickel Cadmium (NiCd), Nickel Metal Hydride (NiMH), Lithium Ion (Li-lon) and Lithium Polymer (Li Polymer), [39].

On the other hand, the disposal of batteries by throwing and burying them in landfills represents a major environmental problem. Where, the batteries hazardous components, i.e., mercury, lead, copper, zinc, cadmium, manganese, nickel and lithium are released, and lead to, pollute both of the soil and the ground water [40].

Of these narrations, at 1987 Micron Sprayers Ltd. (Bromyard, Herefordshire, UK), modified hand-held ULV sprayer, based on the Micro-Ulva [41]. The power supply is provided by 2-8 conventional battery, 1.5V with D size, replacing the fuel. Ultra-Low-Volume "ULV" sprayer intensity, defined as the minimum volume.$area^{-1}$(<5Lha^{-1}) ,with 204 droplets.cm^{-2} of 56.66 to 85.80µm in diameter [42]. Where, the lower amount of the liquids run-off in turn saves the environment and decreases the crop production costs. Using ULV spinning disc sprayer lead to reduce the infestation of white mango scale significantly, and reducing the fungicide amount to < 25%. In addition, it's considered as the most suitable sprayer to control disease plant under local greenhouse conditions [43, 44].

Nevertheless, the main setback of this sprayer type is that the commercially available conventional batteries have operational constraints (it must be changed every 6h, because uncertainty of grid power availability and deep discharge of battery) lead to decreasing on the DC motor rotation speed, poor quality of spray and increasing spraying process cost. Thus, increases the pollution occurring in the soil, and consequently groundwater and waterways [45].

In light of the foregoing narration, to reduce environmental pollution (only and not completely) resulting from the conventional fuels, it is possible to expand in using the renewable energies and rechargeable batteries as a power bank.

This paper aims to process the shortcomings of the regular hand –held ULV spinning cone sprayer "SBD", by converting to a solar-powered sprayer, prolonged the operating time with regularity and at a reasonable cost.

2. Material and Methods

The block diagram of the SSS is shown in Fig.1. It consists of three main units, namely; Energy conversion unit, control unit, and the SBD. The specifics of each unit are discussed below:

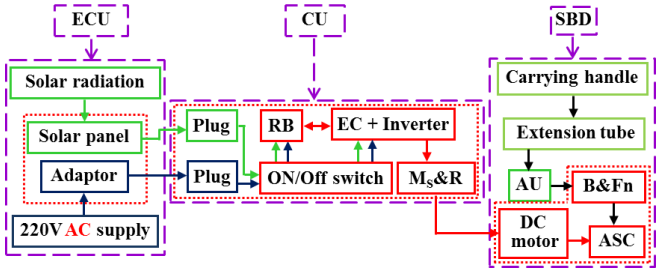

Fig.1: The SSS block diagram.

1- **Energy conversion unit "ECU"**: The energy can be done by three modes; the solar radiation mode "RSM", the rechargeable battery mode "RBM", and the hyper mode "HM".

a- The RSM: The RS obtained from the sun is trapped and converted into electrical energy through SPV. A crystalline silicon (c-Si) type of photovoltaic cell "Pc", with an irregular pentagon shape was used. Two modules of SPV were assembled; SPV_1 with a total area of 2175 cm^2 (cell size ≈ 29 cm^2), for use in the spring and the summer seasons, where, RS ≥ 400 Wm^{-2}. And, SPV_2 with a total area of 3600 cm^2 (cell size ≈ 48 cm^2), for use in the autumn and the winter seasons, where, RS ≤ 400 Wm^{-2}. A 75 Pc was distributed diagonally at a 15 columns connected together in series and parallel as shown in Fig.2.

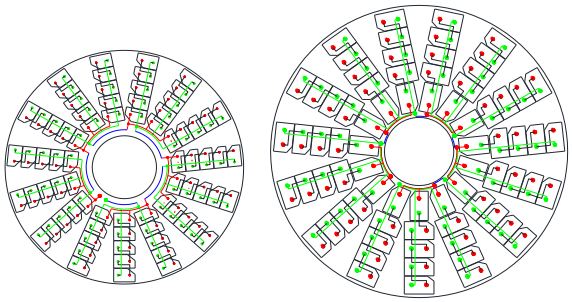

"SPV_1" "SPV_2"

Fig.2: The Pc connections at two SPV modules.

b- The RBM: The electric energy which stored on the chemical form in the rechargeable battery "RB", converting to electrical energy again, to run the sprayer DC motor "SDM". This mode can be used when the RS is not available.

c- The third mode is HM, the electricity is withdrawn automatically from SPV or RB (whichever is greater) to match the electrical power required to perform the SP.

2- Control unit "CU": It includes plugs, RB, electric circuit, inverter, LEDs, switches of; On/Off, and modes "M_S", and regulator "R". The CU is regulating the voltage and controlling the sprayer DC motor rotation speed "S_s"(rpm) through EC, while, the inverter keeps the output power at a constant value. An 8 conventional dry batteries (D) size "CB" were used to predict the relation between the output conventional battery power "CB_P" (W) and S_S (rpm), Fig. 3. Furthermore, R was adjusted at four sets; set 1= the operating power "O_P" was 12 W, and S_S ≈ 3270 ± 5rpm, set 2 = the O_P was 18W and S_S ≈ 4900 ±10rpm and set 3 = the O_P" was 22 W and S_S ≈ 6000rpm. While, N/C set = Charge set at the HM, and = Neutral set, on the RSM and the RBM, where the SSS was operating as SBD (without controlling).

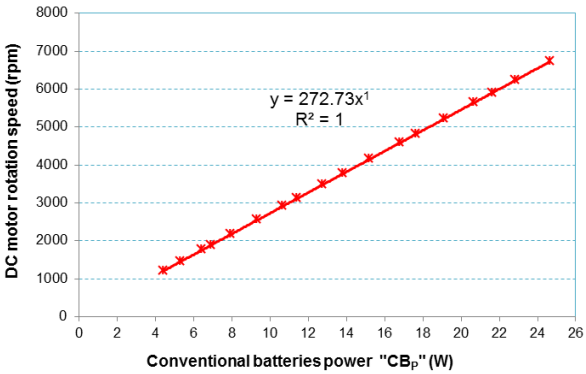

Fig.3: Relationship eq. between CB_P and S_S.

a- **Rechargeable battery "RB":** The SSS was provided with a package of 4 RB, Li- ion battery 18650, 3.7V and 3000mAh, SAMSUNG model. They were connected together in series. Voltage: 14.8V and output power: 44.4W. It used as an alternative power source.

b- **Electric circuit "EC":** It consists of different electronic components. It is provided to charge RB by RS as AC power supply. Also, to changing S_S through regulating the inward voltage (Figs. 4 and5).

c- **LEDs**: An eight LEDs indicates On/off case, modes (RSM, RBM, and HM) and sets (1, 2, 3 and N/C).

3- **Regular hand- held ULV spinning cone sprayer, ULVa+ brand "SBD":** It consists of carrying handle/battery case, extension tube, and the atomizer unit .

a- **Carrying handle/battery case:** It is a cylindrical hollow shape for housing 2-8 CB, with an effective length 60.7cm and 4cm diameter, made of "PVC" (polyvinyl chloride).

b- **Extension tube**: it is a square hallow tube measure 1×1cm, has a low density.

c- **Atomizer unit "AU"**: it includes three items; 1) Bottle and fed nozzle "B&Fn": A liter bottle, made up of PVC. Feed nozzle, with 0.06cm orifice diameter and discharge rate about 0.68 cm^3sec^{-1} was fixed in the bottle bottom. It is converting the spray solution into droplets, designed to replace easily. 2) Atomizer spinning cone "ASC": A grooved toothed cone with volume of 7.80 cm^3, 5.2 and 2.6 cm for cone diameters (upper and lower), and 3cm for height. 3) Sprayer DC motor "SDM": With the following specification; Model: HC315G. Mass: 48.5g. Operating voltage:12V. Free running currant: 2.8A. Torque: 23.81m-NmA^{-1}. Length:

5.1cm. Diameter: 2.75cm. Shaft length: 1.16cm. Shaft diameter: 0.23cm. The ASC was fixed on SDM, as well, AU was fixed on the front end of the extension tube by head locked sleeve, outfitter with three slots to control the spray angle. The overall view of the SSS is as shown in Fig. 6.

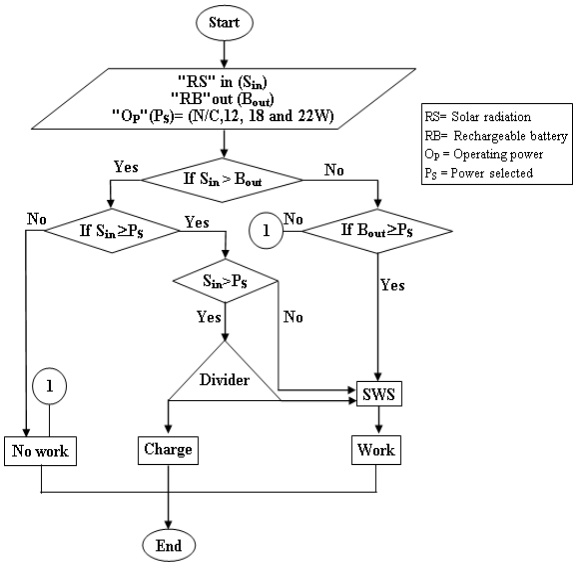

Fig.4: Flowchart

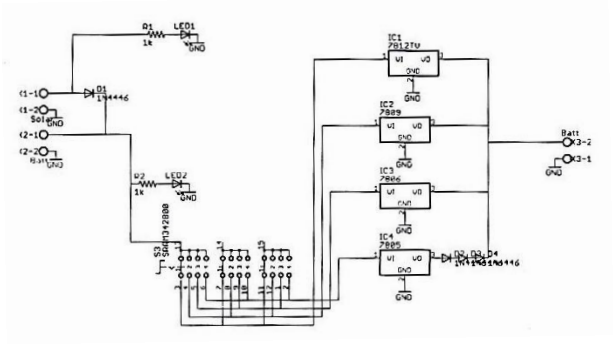

Fig. 5: Electric circuit components arrangement

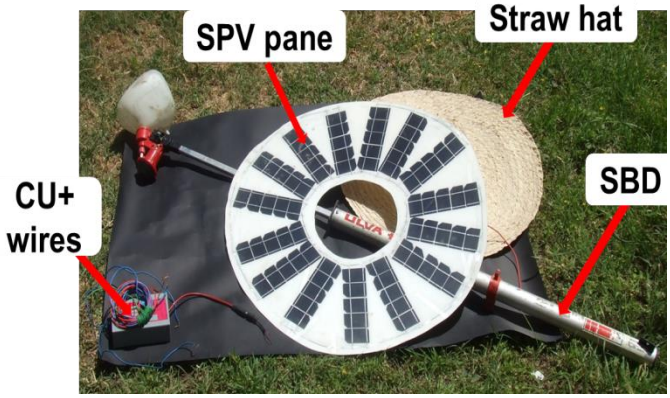

Fig.6: Overall view of the SSS units

Working principle of the SSS:

Basically, there are four cases to supply the electricity:

1- When the sun rays are falling on SPV, a part of the light energy is absorbed and it is converted into electrical energy through Pc by means of electron movements. The SPV delivers an output power, and sends the current to operate SDM, and & or to the Li- ion RB for the storage. Where, RB uses this electricity to charge itself continuously, and the EC limits the rate at which electric current is added to RB, then, battery next is used to operate SDM. The charging process can be done directly by the electrical device. When the switch is turned ON, the electricity is provided to SDM directly from SPV through EC. The SDM can be varied in the larger extent by varying the supply voltage. The sampler circuit on CU samples the output power of SPV into three power levels (12, 18 and 22W), and is connected to SDM. Sprayer liquid reaches to ASC from the bottle through the nozzle by the gravitational force. Where, the nozzle breaks liquid into small droplets. Also, the centrifugal force acting on the ASC by the mechanical power produced by the SDM add velocity to the liquid droplets, and will break it into fine droplets by serrated edges for distribution and deposition on the target plant.

2- In the case of, night operation or the inability of RS to generate sufficient power to operate the sprayer. The operator turned on to RBM. Where, RB provided SDM by electricity, and…etc.

3- If the condition is not satisfied (cloudy weather) the operator turned on to HM. Where, the power value for SPV is compared with RB value. The electricity is withdrawn automatically from SPV or RB (whichever is greater) to match the electrical power required.

4- In case of the RS is not enough to operate SSS and RB is depletion. It can be operated directly by an AC electrical source through an adaptor.

The current study was conducted in two stages:

1) A pre – experiment: The overall objective of it;

a- Evaluating performance of the SSS at RBM, with different sets, through determining both of the rechargeable battery operating time "RBOT"(h) and S_S (rpm). Casio digital stop watch, JHS model, with1/100sec. accuracy, and a digital tachometer, combination (contact/ photo) with ± 5% accuracy were used. This procedure was repeated 3 times.

b- Analyzing the data obtained from the Egyptian Meteorological Authority "EMA", for Cairo governorate of the climatic season 2018-2019. This, begins at the winter season on 21/12/2018 till, the end of the autumn season on 20/12/2019. To get the preliminary vision of the SSS operating ability under, the lowest day of solar radiation in the winter season "LDW" and the sunniest day in the summer season "SDS", through recording the RS values.

c- Performing some theoretical calculations, i.e., the maximum power generated on the SPV surface at different RS "SPV_P" (W), the area of the SPV "SPV_a" (cm^2), and confining the solar operating time "SOT" at different sets. As well as, predict charging time "CT" (h) and charging percentage "CP" (h) for RB. Lastly, prognosticate, the backup operating time "BOT" (h) supported by RB for operating SSS after nightfall or at cloudy days and total operating time "TOT" (h) at HM, were calculated according to heirafter equations as described by [46, 33,47,48,49].

$$SPV_P = V \times I$$

$$SPV_a = \frac{SPV_P}{RS \times \eta}$$

$$CT = \frac{RB_P \times SOT}{SPV_P - O_P}$$

$$CP = \frac{SOT}{CT} \times 100$$

$$BOT = \frac{RB_P \times SOT}{O_P \times CT}$$

$$TOT = SOT + RBOT + BOT$$

Where: V, and I, are voltage (V) and current (A) at maximum power; RS, solar radiation (Wm^2); η, "Pc" eff. (≈19.25% according factory specifications); RB_P, rechargeable battery power (W); O_p, operating power (W); and RBOT, rechargeable battery operating time (h). All electric measurements, i.e., current amber and voltage, were measured by HANDSKIT DT- 9205A digital multimeter brand DEXLE. Where, the current produced by the SPV can be measured by connecting an ammeter in series with the supply.

2) Main experiments: These experiments were carried on Agic. Eng. Fac., Al- Azhar Univ., Cairo, Egypt., workshops, during 2020. It included;

a- Determining TOT items i.e., RBOT, SOT and expecting BOT for the HM, and only SOT determined for the RSM. In addition, calculate both of CT and CP on HM, by using SPV modules at different sets. With assuming that, the RB will recharge with 100% of their capacity.

b- Technical evaluation: The SSS performance at different modes and sets was evaluated through a horizontal coverage test which described by [44]. The spectrophotometer wavelength 320-1000nm with ±2% accuracy was used to assess the amount of the dye on each strip. The experiment of each mode and sets were operated for 3min and were conducted in five replications.

The data were collected at 17/12/2020 (from 10:15 to 13:45), for the RSM, and at 27/12/2020 (from 11:30 to 14:10), for the HM. Solar power meter, model SPM- 1116 SD was used to measure the RS, through 24h. Later, the generated data from the coverage test were subjected to analysis statistically delineation in randomized block design, to calculate analyses of variance (ANOVA) according to the procedure of [50]. Followed by the LSD-test, with significance level 95 and 99%. Also, the coefficient of variation "C.V." (%), as a variation measures for the DDI at each measuring point was calculated.

c- Techno economical cost: The power cost "P_{co}"(LEh^{-1}) of the SSS at the HM with set 1 "F" is calculated and its value is compared with different operating cases, i.e., "A": operating by CP, "B": operating by RB, "C": operating by RB&CU, "D": operating by RS and "E": operating by RS&CU without RB. The "P_{CO}" was calculated according to [51], with exclusion overhead cost and TSII (Rate of taxes, shelter, insurance, and interest) values from fixed cost, and considering that the power source prices (CB, RB and RS), are the only variable items in this equation. The P_{co} at different cases were calculated according hereafter equations:

$$A = \frac{N_B \times G}{T_B}$$

$$B = \frac{N_B \times RB_g}{L} + RC_c$$

$$C = B + CU_G$$

$$D = \frac{SPV_g + A_g}{L}$$

$$E = D + CU_G$$

$$F = E + \frac{N_B \times RP_g}{L}$$

Where: N_B= No. of batteries; G = Price of conventional dry battery (LE); T_B = Operating time for CB; PB_g = Price of RB (LE); L= Operating life of RB (h); RC_C = Recharging cost for RB (assuming ≈ 0.38 LEh^{-1}); CU_g = Price of control unit (including EC, Inverter, control box, and wires,LEh^{-1}) ;SPV_G=Price of SPV (LE); and A_g=Price of straw hat and wires, (LE).

3. Results and Discussion

3.1 Pre – experiment results

3.1.1 The SSS performance at RBM

The performance of the SSS (O_p and S_S) at RBM was represented in fig.7. On the N/C set, the SSS drains RB_p in an irregular manner. It consumes more than 35.84W through 18h of continuous RBOT. Where, it consumes about 13.53W with rate of 2.25Wh^{-1}, at the beginning of the first 6h. Then, 10.53W at a rate of 1.76Wh^{-1}, at next 6h. And finally 7.4W at a rate of 1.23Wh^{-1} until operation end (18h of RBOT). Furthermore, S_S curve, also, decreased paralleled with the O_P curve by increasing RBOT. Where, there is a wide variation in S_S during RPOT. It was observed that S_S drops from 12090 ± 10 rpm at start-up, to 2330 ± 5 rpm after 18h of the RPOT. The S_S decreases about 30.49, 36.67 and 46.36% at every six hours of RPOT respectively. From the above results, it can be concluded that, there is a negative linear relation that governs the SSS behavior through RBOT. The previous relations were fitted to the following equations; S_S =-537.5 (RBOT)+11634, with R^2 (0.99), and O_P =-1.9814 (RBOT) + 42.844, with R^2(0.99). These previous results are directly reflected in the droplet irregularity (size and distribution). On the other hand, by controlling the SSS through EC and an inverter, it was possible for RB to supply the SSS with constant O_p and S_S for dissimilar times. Where, based on experiments, it is found that, the full charge of RB continuously can run for 3.7, 2.47 and 2.02h on sets 1 (12Wand 3270 rpm ± 5), 2 (18W and 4900rpm ± 10) and 3 (22W and 6000 rpm), respectively.

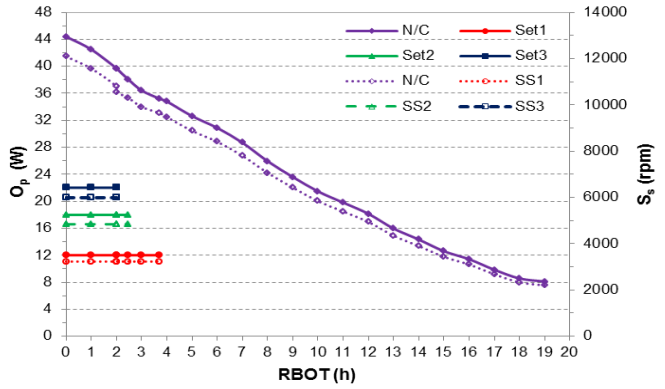

Fig. 7: The SSS performance at RBM

3.1.2 Analyzing climatic data

The first extrapolation of the data obtained from the EMA, during 21/12/2018 till 20/12/2019 that, the lowest value of the RS ≈ 422.01Wm^2 was recorded on the winter season, followed by the autumn season (462.55Wm^2). While, the highest value of the RS ≈ 602.12 Wm^2 was recorded at the summer season (Fig.8).

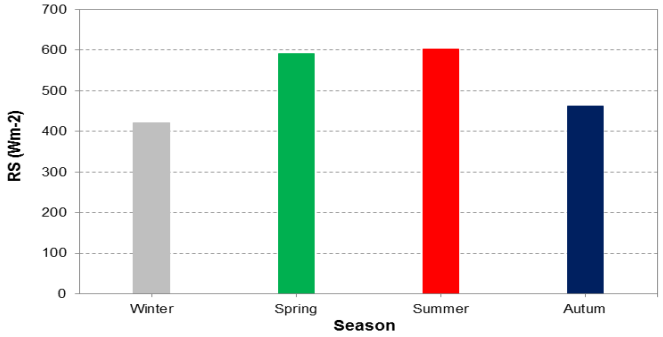

Fig.8: The RS values through climatic seasons 2018-2019.

Likewise, scrutinize the data, and after excluding days with RS < 200 Wm^{-2} (6 days in the winter season, where, the sky is overcast cloudy), it found that, the lowest and highest values of the RS 244.6 and 617Wm^{-2} through 10.1h (from 06:55:00 to 17h: 01min.:00sec.), and 13.7h (from 04:59:00 to 18h: 41min.:00sec.),of daylight, were recorded at the LDW (27/12/2018) and at the SDS (24/5/2019), fig.9. However, the predicting theoretical calculating values of the SPV_P (W), and the S_S (rpm), throughout the "LDW" and the "SDS", were shown at fig.10.

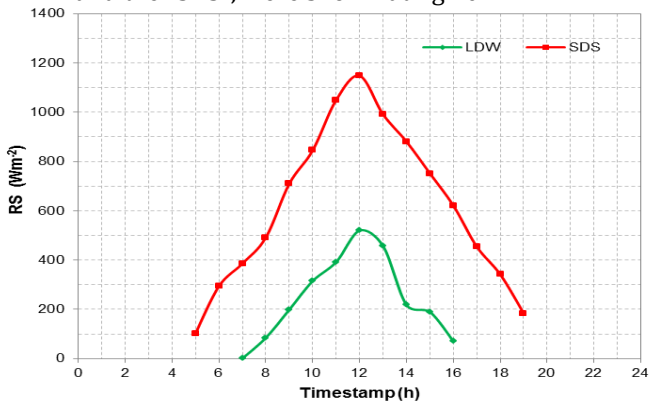

Fig. 9: The RS values through the LDW and the SDS.

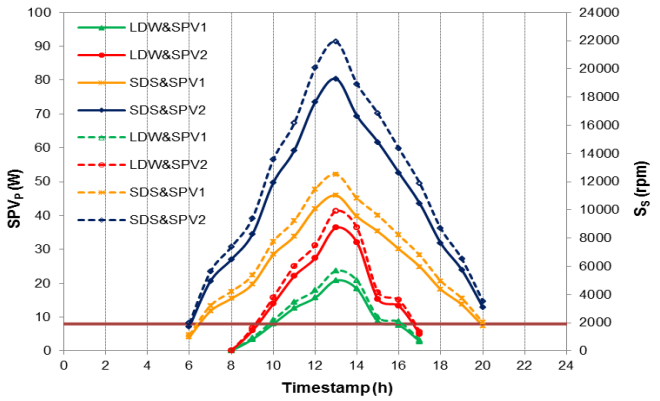

Fig.10: The predicting values of the SPV_P and S_S, at the LDW and the SDS, with SPV modules.

3.1.3 Expecting the "SSS" performance

3.1.3.1 Confining solar operating time, and predicting charge percentage and backup operating time.

Initially, obtained results expected that SPV_1 was unable to operate the SSS at LDW on set 3 (O_p= 22W). Therefore, it is unqualified to recharge RB at any sets. Except, at the N/C set (O_p= 8W), which it could recharge the RB with CP (28.82%) of full capacity. This value of RB_p, enables to extend the SSS operating time "OT" for 1.07h, on set 1(12W), as BOT. On the other hand, in case of using SPV_2 at the SDS, the RB will be recharge during SP with CP of 100% at all sets. This enables RB to extend OT for equal time of RBOT. Where, BOT = RBOT.

Monitoring data, show that, the theoretical values of the SOT, CP, and BOT, were considered as a function of the season, operating set (= O_P) and SPV_a. Where, by analyzing the obtained data it found that, the SOT, CP and therefore BOT at LDW and SDS had been a negative proportion with O_P.

Oppositely, they had a direct relation with SPV_a. Where, increasing O_p from 12 to 22W (set 1 to set 3), and replacing SPV_2 by SPV_1, lead to increasing both of the SOT, CP and BOT at LDW and SDS.

Some logical conclusions could be drawn, based on, climatic data, and substituting its values into theoretical

Table 1: Confining and predicted values of the SOT, CP, and BOT, at different operating sets, for the SPV modules, on the LDW and the SDS.

Time	SPV modules	Operating sets		SOT (h)	CP (%)	BOT (h) at different sets		
		Set	O_P (W)			1	2	3
LDW	SPV_1	N/C	8	6.57	28.82	1.07	--	--
		1	12	3.70	19.81	--	--	--
		2	18	2.68	6.30	--	--	--
		3	22	--	--	--	--	--
	SPV_2	N/C	8	7.39	63.95	3.03	2.02	1.65
		1	12	6.48	54.94	2.03	1.36	1.11
		2	18	4.11	41.42	1.53	1.02	0.84

		3	22	3.41	32.41	1.20	--	--
SDS	SPV_1	N/C	8	13.48	85.43	3.69	2.46	2.01
		1	12	12.29	76.42	2.83	1.88	1.54
		2	18	9.35	62.90	2.33	1.55	1.27
		3	22	8.10	53.90	1.99	1.33	1.09
	SPV_2	N/C	8	14.51	100	3.70	2.47	2.02
		1	12	13.73	100	3.70	2.47	2.02
		2	18	12.79	100	3.70	2.47	2.02
		3	22	12.02	100	3.70	2.47	2.02

predicting equations as follows:

- Operating the SSS on set 3 at LDW& SPV_2, leads to extend the SP for only 1.2 on set 1.
- The maximum value of the SOT ≈ 7.38h at N/C set (O_p= 8W) on the LDW& SPV_2 was less than the minimum value of the SOT ≈ 8.1h at set 3 (O_p= 22W).
- The FCT for RB during SP was also, affected significantly by season. Where, the range of the FCT at LDW (9.92 to 42.57), was more than at SDS (8.92 to 16.08h). (Data not shown).
- On N/C set, the FCT for RB, could be done only during daytime between 09:00:00 to14:39:29, 08:17:18 to 15:40:56, 05:25:28 to 18:53:54 and 05:04:42 to 19h: 35min.: 13sec., at LDW&SPV_1, LDW&SPV_2, SDS&SPV_1 and SDS&SPV_2, respectively. (Data not shown). All previous predictions were tabulated in Table 1.

3.1.3.2 Predicting the total operating time

Where, according paragraph 3.1.1., and analyzing date. The RB is able to operate the SSS with constant O_P of 12, 18, 22W, for about 3.7, 2.47, and 2.02h, respectively, at cloudy days, or before sunshine or even after sunset. The expecting TOT was demonstrated in fig.11.

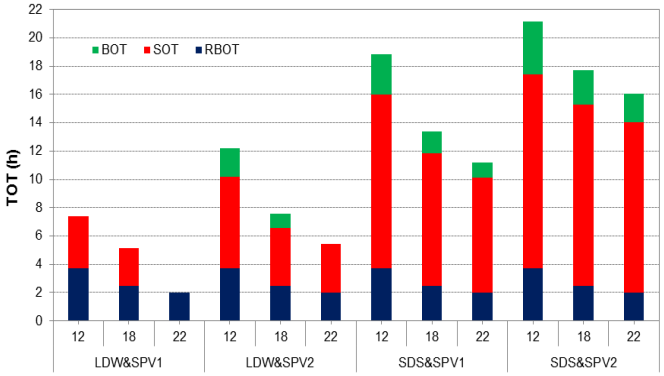

Fig.11: The predicted values of the TOT at the LDW and the SDS with SPV modules.

The RBOT is considered to be the main power source separately at LDW& SPV_1 on set 3. While, the TOT is consists of the RBOT and the SOT only at LDW& SPV_1 on sets 1 and 2, and at LDW& SPV_2 on set 3. Where, RBOT represents about 50 and 47.96 and 37.20% of TOT at the same previous arrangement. However, the operating time by RB, which includes RBOT and BOT, is represents about 46.94, 45.93 and 37.20% from TOT at LDW& SPV_2 on sets 1, and 2. On the other hand, it was reduced to about ≤ 35.02% from TOT at SDS with any SPV modules. These decreases are due to the increasing both of RS intensity and the number of sunshine hours in the summer season.

3.2 Main results

3.2.1 The SSS performance at RSM

The performance of the SSS at RSM, were conducted on Thursday, 17/12/2020, where, the avg. RS ≈ 337.40 Wm^{-2}, with daylight ≈ 10h: 13min. (Sunrise at 6:45, and sunset at 16:58). Where, the SPV_P at midday were 23.36 and 38.94W by using SPV_1 and SPV_2 when, RS was at its peak (556.25 Wm^{-2}), (Fig.12). The highest values of SOT were 7.28 and 7.95h recorded at N/C set by using SPV_1 and SPV_2 modules, (Fig.13). By using SPV_1 the start of SP will be delayed beyond sunrise by about 138, 158, 198 and 266 min. While, operating ends before sunset of 38, 80, 140, and 208 min. on sets N/C, 1, 2 and 3 respectively. Moreover, by using SPV_2 the SP will be delayed beyond sunrise by about 110, 132, 152 and 163min., while, it will be end before sunset of 25, 581, 66 and 88min., at the same previous arrangement. On the other meaning, the SOT affected by SPV_a. Where, it was increased about 00:40:23, 00:48:25, 02:00:31 and 03h: 42min.:49sec. at sets N/C, 1, 2 and 3 respectively, with replacing SPV_2 by SPV_1.

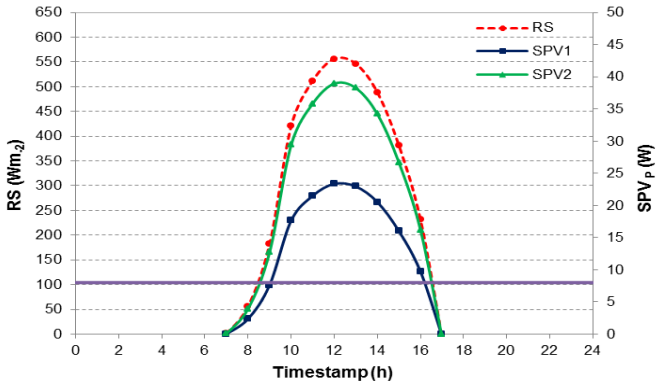

Fig.12: **The** RS and SPV_P on the SPV modules on Thursday, 17/12/2020.

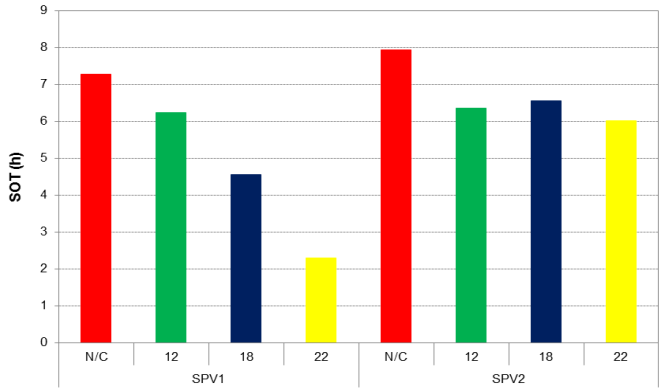

Fig.13: The SOT on the SPV modules with different sets at RSM.

3.2.2 The SSS performance at HM

The performance of the SSS at HM, were conducted on Sunday 27/12/2020, where, the avg. RS ≈ 389.37 Wm^{-2}, with daylight ≈ 10h: 14min. (Sunrise at 6:49 and sunset at 17:03). Where, the SPV_P at midday were 25.34 and

42.24W by using SPV_1 and SPV_2 when, RS was at its peak (603.42Wm^{-2}), (Fig.14).

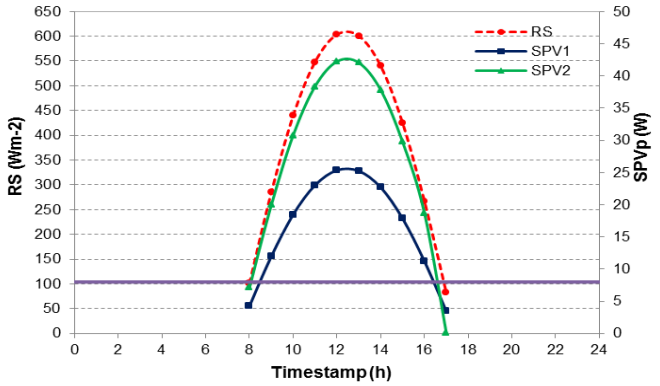

Fig.14: The RS and SPV_P on the SPV modules on Sunday, 27/12/2020.

3.2.2.1 Solar operating time, charge percentage and backup operating time.

Data which derived from Table 2 show that, CP had an opposite relation with O_P and, direct relations with both SOT and SPV_a. These results are as expected on pre – experiment at paragraph 3.1.3.1. Where, increasing O_P from 12 to 22W, and at the same time, decreasing SOT from 6.89 to 3.45h and from 8.04 to 6.57h, resulting in reducing CP from 30.05 to 7.53% and from 68.11 to 45.58%, by using SPV_1 and SPV_2.

Table 2: The values of the SOT, CP and BOT, at different sets for the SPV modules.

SPV modules	Operating sets		SOT (h)	CP (%)	BOT (h) at different sets		
	Set	O_P (W)			1	2	3
SPV_1	1	12	6.89	30.05	0.30	--	--
	2	18	5.06	16.54	--	--	--
	3	22	3.45	7.53	--	--	--
SPV_2	1	12	8.04	68.11	2.52	1.68	1.37
	2	18	7.21	54.59	2.02	1.35	1.10
	3	22	6.57	45.58	1.69	1.12	--

While, it observed that, CP (%) for the RB increased about 97.44,126.66 and 230.05% at 12, 18 and 22W respectively, with replacing SPV_2 by SPV_1. With using SPV_1, only, 06h: 53min: 23sec.(6.89h), of the SOT on set 1, is able to recharge RB with CP about 30.05%. This value is sufficient to extend the operating time of the SSS on the same set for another 30min., as BOT. Meanwhile, with using SPV_2, the values of CP for RB (68.11, 54.59 and 45.58%) , due to 8.04, 7.21, and 6.75h of SOT, on O_p of 12, 18W and 22W are plenty to increase SP operating time for dissimilar time as BOT depending on O_p" as tabulated at previous table.

3.2.2.2 The full charge time

Based on experiments, with using SPV_1 it is found that the recharged process can be done during day time between 8.19 to16.25, 9 to 15.53, 9.55 to 14.58, and 10.43 to 14.10 on set N/C, 1, 2 and 3 respectively. However, with using SPV_2, the recharged process can be done through 08:33:14, 08:02:39, 07:12:24 and 06h: 34 min.:16 sec., at the same prior set arrangement. On the other hand, there were direct relations between O_P and FCT. Where, by using SPV_1 and SPV_2, and turning O_P from set N/C (8W) to set 3, the FCT were increased from 20.35 to 45.86h and from 11.09 to 14.41h. Practically, with replacing SPV_2 by SPV_1, it was observed that, FCT or necessary time for charging the RB of 12.5V, 3Ah, was decreased about 68.58, 56.85, 48.54, and 45.50 % at the O_P of 22, 18, 12 and N/C set respectively. These may be due to increased PVC_a, (Fig.15). Similar observations were found as [52].

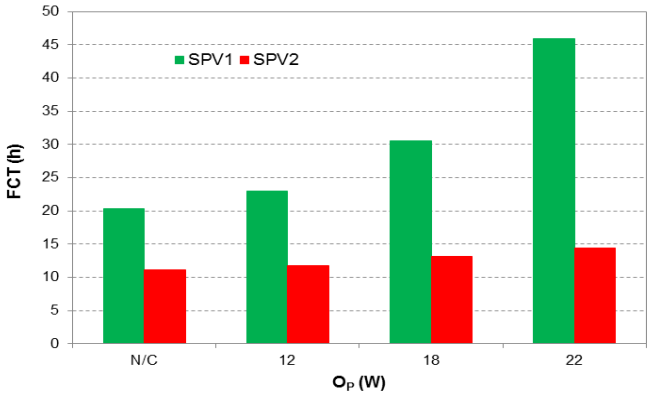

Fig.15: The FCT for 4 RB by SPV modules.

3.2.2.3 The total operating time

The demonstrated data which represented graphically in Fig. 16 show that, generally, the TOT by using the SPV_2 module is more than using the SPV_1 module, with a rate of 30.89, 46.44 and 56.92% at O_P of 12, 18 and 22W respectively. The TOT reduced about 30.87 and 49.75 by increasing the O_p from 12 to 18 or to 22W with using SPV_1. While, it is reduce about 22.33 and 22.11% by increasing the O_p from 12 to 18W and from 18 to 22W. Both of SPV modules were unable to recharge RB during SP, with two following exceptions; First one, extended the SP time on set 1 for another 30min., by operating the SSS on set 1 (12W) with using SPV_1. Second exception, expanded the SP time on set 2 and 3 for another 252 and 95 min., as BOT. by operating the SSS on set 1 and 2, with using SPV_2. The OT by RB (RBOT + BOT) represented about 36.72, 43.63 and 34.64% from TOT for just previous cases. Meanwhile, RBOT represented about 32.80 and 36.90% of TOT by using SPV_1 on set 2 and 3, and only 23.52% by using SPV_2 on set 3. All, previous results were in harmony with those obtained by [53].

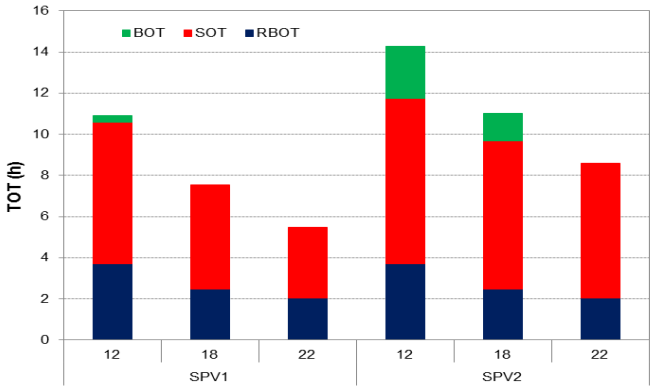

Fig.16: The TOT at different sets, with the SPV modules on HM.

3.2.2.4 Technical evaluation (Droplet deposition intensity)

Distribution uniformity or droplet deposition intensity "DDI"(μgm^{-2}) across coverage area is a measuring performance factor relating to SSS technical evaluation [44]. As can be seen from Fig. 17 there is one peak is directly below the nozzle, and there is almost homogeneity between the DDI in the right and the left of the operating axis. Moreover, results show that there is almost congruence between the curves of the different operating modes with the same S_S. In addition to, by increasing S_S from set 1 to sets 2 and 3 at different operating mods lead to decrease the curve height, and increase the breadth of the curve base (horizontal covered area). These results advocated by [54, 2]. Where, the obtained results indicated that, the SSS on set 1 performed the highest average DDI

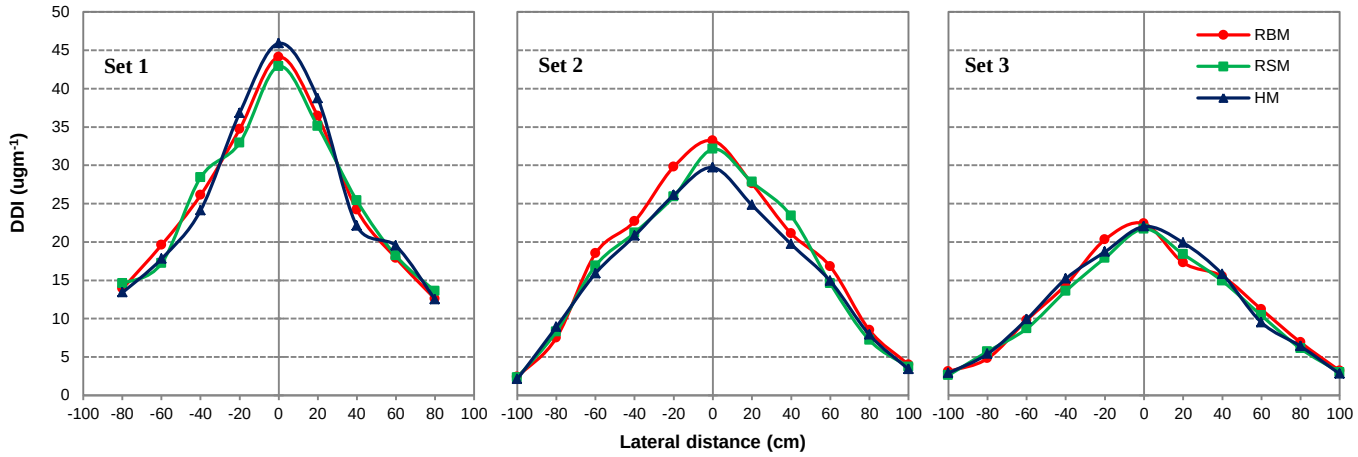

Fig. 17: The technical evaluation of the SSS performance through on different sets and modes.

were 44.1, 42.9 and 45.9 (μgm^{-2}) at center axis of SP at RBM, RSM and HM respectively. Meanwhile, the lowest DDI (22.4, 21.7 and 22 μgm^{-2}) were gained on set 3 at the same previous operating mode arrangement. On the other hand, the lateral distance was increased from ±80cm at set 1 to ±100cm at set 2 and 3. In general, this data was in agreement with those obtained by [55]. This indicates that with increasing S_S, the uniformity and homogeneity of DDI coverage improved. The similar observation had been marked by [6, 56]. Finally, results affirmed that, the coefficient of variation (%) of DDI ≤ 10% at all position of lateral distance on different sets and mods. Of late results, the SS has a height significant effect (P ≤ 1%) on the DDI, while, the operating mode was insignificant.

3.2.2.5 Techno economical cost:

The detailed cost of different components of the SSS is represented in Table 3. Meanwhile, the power cost "P_{CO}" (LEh^{-1}) of the SSS at different operating cases, were calculated and its value is compared with SBD operating cost and plotted at Fig.18.

Table 3: Detailed cost of all the major components, in Egyptian currency, and operating time for the SSS.

Item	Units	Unit price (LE*)	Operating time (h)
Conventional Battery "CB".	8	15	6**
Rechargeable battery "RB".	4	80	4380 or 2496.6***
SPV panel.	1	500	76096****
Straw hat .	1	75	4234
Electric wires.	5m	2	
Electric circuit "EC".	1	450	19024
Inverter.	1	300	
Control box (box + LEDs + switches)	1	50	

*1LE=0.0639$ (10/4/2021), **According[57]., ***According operating case., **** Yearly operating time for SPV, it is only 328 day year^{-1} with 11.6hday^{-1} as an average actual daylight hours, after excluding overcast or partially cloudy days (37days), according EMA.

All replacement power sources at different cases were more less than operating the SBD by CP. Where, the P_{CO} decreased very sharply from 20LEh^{-1} at SBD to less 1 LEh^{-1} for all other cases of the SSS. As well, it reach to 0.45, 0.55, 0.02, 0.06 and 0.19LEh^{-1} with B, C, D, E and F cases, respectively.

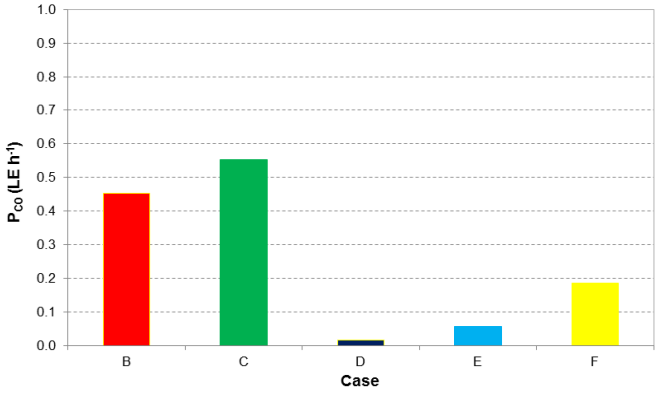

Fig. 18: The P_{CO} of the SSS at different operating cases.

Another, conclusion from the same figure is the P_{CO} for the SSS reduced with using RS comparing with RB at different cases. Where, it reduced from 0.45 at case B to 0.02 LEh^{-1} at case D, with a rate of 96.52%, and from 0.55 at case C to 0.06 LEh^{-1} at case E, with a rate of 89.54%.

On the other hand, increasing P_{CO} about 0.1 and 0.04 LEh^{-1} from cases C to B, and from E to D, due to the CU cost, had a positive effect on the SSS performance. Where, the performances at B and D cases were similar as SBD, and characterized by, irregularity of spraying and losses a high amount of the sprayed substance. These, leads to re-spraying process in order to avoid major losses in the yield, thus, increasing the spraying cost.

Finally, with deep looking at the same figure, in spite of, the case F had a higher P_{CO} (0.19 LEh^{-1}) comparing with other two RS cases (D and E), but it prefers all of them.

Where, its performance described as regularity in distribution, because it isn't affected by the season, RS, time of day and it is always available in use, even at cloudy days. In addition, it had long TOT due to support time provided by RBOT and BOT, with saving the RC_C. At the last, it found that, the initial cost for SSS (including price of RB, SPV, EC … etc.), is very high about (1465 LE). Where, it is represented about 3– 4 times of the SPD price (about 395 LE). But, with use of new technologies to enhance SPV conversion eff., by innovations multiple cells with different bands. Besides, using low cost material and mass production, may make the SPV more inexpensive. On the other hand, advantages of solar energy, i.e., very less running cost, eco-friendly and it is very much helpful in a distant places, make SSS attractive [58,59,60].

4. Conclusion

The main target of the study was to develop the SPD to a solar powered sprayer system "SSS". For this purpose, the SPD was developed by adding CU and SPV. Based on experiments, the SP can be done without the SPV on constant O_P of 12, 18 and 22W, for a minimum period of 3.7, 2.47, and 2.02 h, respectively. Moreover, it is found that the recharged process for the RB (which considered as power bank), can be done separately or during SP. The TOT for SP had an opposite relation with the O_P, and direct relations with both of the SOT and the SPV_a, in contrary of the RB full charge time. Also, results show that there is almost congruence between the DDI curves on the different operating modes at the same S_S. Besides, the O_P has a height significant effect on the DDI, while, the operating mode was insignificant. Finally, it can be concluded that the SSS is eco-friendly & pollution free, with regularity distribution, and had long TOT. Likewise, the P_{CO} of it was more economical. Where, the running cost is very less and the maintenance cost is only restricted to operating life of the RB and SPV. On the other hand, as a future scope, the BOT for the RB can be increased by adopting some new technology in electronic fields (PWM techniques).

5. References

[1] H. Zhu, Y.Jiang, H. Li, J. Li, and H. Zhang. Effects of application parameters on spray characteristics of multi-rotor UAV. Int. J. Precis Agric. Aviat., 2 (1) pp. 18- 25, 2019.

[2] J. P. Sinha, J. K. Singh, A. Kumar, and K.N. Agarwal. Development of solar powered knapsack sprayer. Indian Journal of Agricultural Sciences, 88 (4) pp. 590–595, 2018.

[3] E.C. Oerke. Crop losses to pests. The Journal of Agricultural Science 144 pp. 31-43, 2006.

[4] H. Jain, N. Gangrade, S. Paul, H. Gangrade, and J. Ghosh. Design and fabrication of solar pesticide sprayer, IJARIIE., 4 (2) pp. 1715- 2727, 2018.

[5] D. Nuyittens, M. De.Schampheleire, P. Verboven, E. Brusselman, D. Dekeyser. Droplet size and velocity characteristics of agricultural sprays. Transactions of the ASABE., 52 pp.1471-1480, 2009.

[6] V. Swami, D. K. Chauhan, P. Santra, and K. Kothari1. Design and development of solar PV based power sprayer for agricultural use. Annals of Arid Zone, 55 (1&2) pp. 51-57, 2016.

[7] A.A.I. Mohamed. Evaluation of the current ground spraying techniques used for controlling cotton insects in Egypt. Misr J. Eng., 15 (3) pp.534-544,1998.

[8] M.A. Moharum, and N. M. El-bialee. Control of the white mango scale. (Aulacaspis Tubercularis) using ultra low volume (ULV) and gun motor sprayers. Egypt. J. Agric. Res., 93 (5B) pp. 611-623, 2015.

[9] V.V. Rao, S. Mathapati, and B. Amarapur. Multiple power supplied fertilizer sprayer. International Journal of Scientific and Research Publications, 3 (8) pp.1-5, 2013.

[10] A.P. Patil, S.V. Chavan, A.P. Patil, and M.H. Geete. Performance evaulation of solar operated knapsack sprayer. Indian Journals, 38(3) pp. 15-18, 2014.

[11] P.V. Sawalakhe, A. Wandhare, A. Sontakke, B. Patil, R. Bawanwade, and S. Kurjekar. Solar powered seed sowing machine. Global Journal of Advanced Research, 2(4) pp. 712-717, 2015.

[12] S. Kshirsagar , V. Dadmal, P. Umak, G. Munde, and P.R. Mahale. Design and development of agriculture sprayer vehicle. IJCET., 4 pp. 405-408, 2016.
[13]V.M.Magar, G. Gade, S. Salve and V. Vora. Development of portable solar operated pesticide sprayer, 2017. Global Research and Development Journal for Engineering, 2 (6) pp. 237-241, 2017.
[14] W.A. Issa, B. Abdulmumuni, R.O. Azeez, I.N. Okpara, J.O. Fanifosi, and O.B. Ologunye. Design, fabrication, and testing of a movable solar operated sprayer for farming operation. IJMET., 11 (3) pp. 6-14, 2020.
[15] B. Poudel, R. Sapkota, R. B. Shah, N. Subedi, and A. Krishna. Design and fabrication of solar powered semi-automatic pesticide sprayer. IRJET., 4 (7) pp. 2073-2077, 2017.
[16] S.R. Bull. Renewable energy today and tomorrow. Environmental Sciences and Pollution Management: Proceedings of the IEEE, 89 (8) pp. 1216-1226, 2001.
[17] M. Sobhani, S. Zakeri, and M. M. Taghizadeh. Review on renewable energy, sustainable energy and clean energies. Tech. J. Engin & App. Sci., 4 (3) pp. 120-123, 2014.
[18] A. Mehmood, Waqas and H.T. Mahmood. Economic viability of solar photovoltaic water pump for sustainable agriculture growth in Pakistan. Materials Today Proceedings, 2 pp. 5190- 5195, 2015.
[19] J. Mohtasham. Review Article-Renewable Energies. International Conference on Technologies and Materials for Renewable Energy, Environment and Sustainability, TMREES15. Energy Procedia, 74 pp.1289 – 1297, 2015.
[20] I. Daut, N.Gomesh, M. Irwanto, and Y.M. Irwan. Energy saving suction hood. World Academy of Science, Engineering and Technology, 6 (1) pp. 612-616, 2012.
[21] K. Bataineh, and Y. Taamneh. Review and recent improvements of solar sorption cooling systems. Energy Build, 128 pp. 22–37, 2016.
[22] V. Koli, Sudham, V. Kumar, S. Patil, and K.S. Badarinarayan. Solar agro sprayer with night vision. IRJET., 3(6) pp. 1128-1130, 2016.
[23] A.S. Shriwaskar, S.M. Lonkar, A.M. Tarale, R.R.Deoghare, and P.B. Malve. Custamized solar sprayer. IJAERD., 3 (3) pp. 201-209, 2016.
[24] M.V. Torshizi, and A. H. Mighani. The application of solar energy in agricultural systems. JRESD., 3 (2) pp. 234-240, 2017.
[25] M.N. Comsan. Solar energy perspectives in Egypt, Proceedings of the 4th Environmental Physical conference,10-14 March 2010, Hurghada, Egypt, pp. 1-11. 2010.
[26] H.S. Abdel-Galil. Solar system with energy storage for drying poultry manure. Misr, J. Ag. Eng., 24 (4) pp. 978-1003, 2007.
[27] A. Ibrahim. Renewable energy source in the Egyptian electricity market: A review. Renewable and sustainable. Energy Reviews, 16 (1) pp. 216-230, 2012.
[28] A. Jivrag, V. Chawre, and A. Bhagwat. Solar operated multiple granulated pesticide duster. Proceedings of the World Congress on Engineering, 3. London,U.K., 2011.
[29] S. Roblin. Solar-powered irrigation: A solution to water management in agriculture. Renewable Energy Focus, 17 pp. 1-12, 2016.
[30] S. Poonia, D. Jain, P. Santra and A.K. Singh. Use of solar energy in agricultural production and processing Indian Farming, 68(09) pp.104–107, 2018.
[31] W.M. Mohamed. Evaulation using solar energy for operating disk mower in one of new vally farms. M.Sc., Thesis, Agric. Eng., Fac. of Agric., Ain Shams Univ. Egypt., 2019.
[32] T.M, Salem. Using solar energy for pumping water in drip irrigation system. J. Soil Sci. and Agric. Eng., Mansoura Univ., 9 (1) pp.1-17. 2019.
[33] A.A.M. Taie. The use of solar energy for operating small stationary agricultural machines. M.Sc., Thesis, Agric. Eng., Fac. of Agric., Ain Shams Univ. Egypt., 2019.
[34] R. Borah, F.R. Hughson, J. Johnston, and T. Nann. On battery materials and methods. Materials Today Advances, 6 pp. 1- 22, 2020.
[35] Z. Khan. Unique solar operated spray jet. IOSR - JMCE pp. 43-46, 2014.
[36] S. Sabihuddin, A. E. Kiprakis and M. Mueller. A numerical and graphical review of energy storage technologies. Energies, 8 pp.172- 216, 2015.
[37] D.E. Von Handorf. The Baghdad Battery—Myth or Reality?. Plating & Surface Finishing. Pp. 84-87, 2002.
[38] A.M.Bernardes, D.C.R. Espinosa, and J.A.S. Tenório. Recycling of batteries: a review of current processes and technologies. Journal of Power Sources, 130 pp. 291–298, 2004.
[39] O. Peter, T.S. David, B. Godfrey, and M. Jehold. Comparison of the efficiency of R20 (D-size) dry cell battery brands used in Uganda. International Journal of Electrical and Electronics Research, 8 (2) pp. 38-41, 2020.
[40] W.S. Chena, C-T. Liao, K-Y Lina. Recovery Zinc and Manganese from spent battery powder by hydro-metallurgical route. 3rd International Conference on Energy and Environment Research, ICEER 2016, 7-11September 2016, Barcelona, Spain. Energy Procedia, 107 pp. 167–174, 2017.
[41] N. D. Jago, and P. A. Shah. Description of a modified hand-held ultra-low-volume sprayer for millet crop protection by Sahelian farmers. Tropical Pest Management, 37(2) 129-131, 1991.
[42] M.S.H. Moustafa , and A.A. Ismail. Effect of fungicide applicator types on the efficacy of fungicides used for control late blight of potato. J. Agric. Res. Tanta Univ., 29(3) pp. 568-576, 2003.
[43] A.A. Ismail, and S.E. Badr. Effect of some applicator types on metalaxyl residue in cucumber with special reference to its toxicological effects. Minufiya J. Agric. Res., 2 (29) pp. 557-568, 2004.
[44] A.S. El-Ashry, H.A. El-Gendy, and M.H. Abo El-Naga. Development and performance evaluation of a greenhouse pesticide sprayer. The 16th. Annual Conference of the Misr Society of Ag. Eng., 25 July, 2009 pp. 466 -1477, 2009.

[45] P. Tamilselvi, and A.D. Krishnan. Ergonomic evaluation of conventional agricultural sprayers with respect to human performance. Agriculture Science Digest., 36(3) pp. 179–84, 2016.
[46] M.S. Sawant, S.S. Nimbalkar, A.P. Yadav, D.A. Bondge, and M. M. Patil. Multiple power supplied fertilizer sprayer. IJIERT., 2 (2) pp. 1-6, 2015.
[47] M.S. Teja, N.K. Kumar, P. H. Kumar, and G. Singaiah. Solar Fertilizer Spray. International Journal & Magazine of Engineering, Technology, Management and Research, 4 (8) pp. 203-207, 2017.
[48] A. Nawaz, L. R. Dsouza, A. Kumar, M. Tabrez, and S. Rao K.. Design and fabrication of hybrid multipurpose solar sprayer. IJERMCE., 2 (4) pp. 726- 730, 2017.
[49] K.B. Murthy, R. Kanwar, I. Yadav and V. Das. Solar Pesticide Sprayer. IJLERA., 2 (5) pp. 82-89, 2017.
[50] K.A. Gomez, and A.A. Gomez. Statistical Procedure for Agricultural Research, 2nd ed. John Wiley and Sons Inc., Croda. 1984.
[51] FMO. Fundamental of machine operation. Johan Deere Company, Moline, Illinois. 2ed. USA.,Pp: 94-102, 1975.
[52] R.S. Sasaki, M. M. Teixeira, D. O. Filho, C.J. Cesconetti, A. C. Silva, and D. M. Leite. Development of a solar photovoltaic backpack sprayer. Comunicata Scientiae, 5(4) pp. 395-401, 2014.
[53] N.S. Wade, and T.D. Short. Optimization of a linear actuator for use in a solar powered water pump. Solar Energy, 86 pp. 867- 876, 2012.
[54] C. Zhai, Z. Chunjiang, W. Xiu, L. Wei, L. Wei, and Z. Ruixiang. Nozzle test system for droplet deposition characteristics of orchard air-assisted sprayer and its application. Int. J. Agric & Biol. Eng., 7(2) pp.122-129, 2014.
[55] M.S.H. Moustafa, A.A. Ismail., and H.A. El- Gendy. Effect of fungicides applicator -types on fungicide efficiency and environmental pollution. The11th Annual conference of Misr Society of Agr. Eng., pp. 735-746, 2003.
[56] Z. Hang, Y. Jiang, H. Li, J. Li, and H. Zhang. Effects of application parameters on spray characteristics of multi-rotor UAV. Int. J. Precis Agric. Aviat., 2(1)pp. 18-25, 2019.
[57] H.A. El- Gendy. A study on the operation of an Ultra-Low-Volume sprayer bu solar photovoltaic cells. M.Sc., Thesis, Agric. Mech., Fac. of Agric., Ain Shams Univ. Egypt. 1994.
[58] F. Dinçer. The analysis on photovoltaic electricity generation status, potential and policies of the leading countries in solar energy. Renewable and Sustainable Energy Reviews, 15 pp.713-720, 2011.
[59] M.E. Meral, and F. Dinçer. A review of the factors affecting operation and efficiency of photovoltaic based electricity generation systems. Renewable and Sustainable Energy Reviews., 15pp. 2176–2184, 2011.
[60]A. Mishra, N. Bhagat, and P. Singh. Development of solar operated sprayer for small scale farmers. International Journal of Current Microbiology and Applied Sciences. Int. J. Curr. Microbiol. App. Sci., 8 (2) pp. 2593-2596, 2019.